

# Dynamics of spatial Fourier modes in turbulence

## Sweeping effect, long-time correlations and temporal intermittency

C. Poulain<sup>1,a</sup>, N. Mazellier<sup>2</sup>, L. Chevillard<sup>2</sup>, Y. Gagne<sup>2</sup>, and C. Baudet<sup>2,b</sup>

<sup>1</sup> Commissariat à l'Énergie Atomique (CEA), 17 rue des Martyrs, 38054 Grenoble, France

<sup>2</sup> Laboratoire des Écoulements Géophysiques et Industriels (LEGI), 38041 Grenoble, Cedex 9, France

Received 13 April 2006 / Received in final form 28 June 2006

Published online 27 September 2006 – © EDP Sciences, Società Italiana di Fisica, Springer-Verlag 2006

**Abstract.** We present the results of an experimental study of the spatial Fourier modes of the vorticity in a turbulent jet flow. By means of an acoustic scattering setup we have recorded the evolution in time of Fourier modes of the vorticity field, characterized by well defined wavevectors  $\mathbf{k}$ . By computing the auto-correlation of the amplitude of the Fourier modes we evidence that, whatever the length scale (or equivalently  $\mathbf{k}$ ), the dynamic evolution of the vorticity field involves two well separated time scales. We have also performed the simultaneous acquisitions of pairs of Fourier modes with two wavevectors  $\mathbf{k}$  and  $\mathbf{k}'$ . Whatever the spectral gap  $\mathbf{k} - \mathbf{k}'$ , any pair of Fourier modes exhibits a significant cross-correlation over long time delays, indicating a strong statistical dependence between scales.

**PACS.** 47.27.Gs Isotropic turbulence; homogeneous turbulence – 47.32.C- Vortex dynamics – 43.28.+h Aeroacoustics and atmospheric sound

## 1 Introduction

Statistical intermittency remains one of the main puzzling features of turbulence, still unresolved [1]. At the experimental level, following Kolmogorov initial prediction [2], the scale evolution of the turbulence statistical properties can be traced by computing the spatial velocity increments,  $\delta u_r(\mathbf{x}, t) = u(\mathbf{x} + \mathbf{r}, t) - u(\mathbf{x}, t)$ . Usually, one resorts to hot-wire anemometry providing Eulerian measurements of the longitudinal velocity component at one point  $\mathbf{x}_o$  along time  $t$ . Scale dependence is then recovered by mapping time increments  $\delta t$  of the Eulerian signal onto spatial increments  $r = -U_{avg}\delta t$  according to the Taylor hypothesis of *frozen turbulence* [1]:  $\delta u_r(t) = u(\mathbf{x}_o, t) - u(\mathbf{x}_o, t - r/U_{avg})$ . In this paper, we present an alternate way to experimentally study statistical scale dependence in turbulent flows, relying on a direct spatial Fourier analysis of the vorticity field. Since the vorticity field is the curl of the velocity field, in the Fourier domain where  $\tilde{\omega}(\mathbf{k}, t) = i\mathbf{k} \times \tilde{\mathbf{u}}(\mathbf{k}, t)$ , one expects similar statistics for the amplitudes of the Fourier modes of vorticity and velocity [3]. The temporal evolution of spatial Fourier modes of the turbulent vorticity field  $\tilde{\omega}(\mathbf{k}, t)$  are obtained by an acoustic scattering technique which allows the direct selection of a well defined spatial wavevector  $\mathbf{k}$  [3,4]. Indeed, spectral measurements, based on wave scattering

experiments are commonly used in various domains of research in physics, starting with phase transitions and critical phenomena in condensed matter physics where light and neutron scattering techniques are largely widespread.

According to Kolmogorov *refined similarity hypothesis* [1,5], statistical intermittency of turbulent flows is the consequence of the strong spatial heterogeneity (possibly multifractality) of the local energy dissipation rate, related to some kind of multiplicative cascade process of the kinetic energy across scales. The energy dissipation rate is also expected to display strong time fluctuations, possibly reflecting unavoidable temporal fluctuations of the large-scale forcing processes [6]. Recently, it has been suggested [7], that the study of dynamical multiscaling (time dependence of the velocity structure functions) could be of valuable help for a better comprehension of turbulence intermittency. Unfortunately, as implicitly stated by the Taylor hypothesis, the statistics of Eulerian velocity increments are strongly dominated by the spatial features of the flow and thus, weakly sensitive to its temporal fluctuations. Actually, it is generally accepted that the latter fact is a direct consequence of the random character of the advection by the large scale flow, past any Eulerian probe, of the whole velocity field (the so-called sweeping effect [8–12]). It is worth noticing that in wave scattering experiments (whatever sound or light), thanks to the direct spatial Fourier transform involved in the scattering process, the length scale selection is realized by the choice

<sup>a</sup> e-mail: cedric.poulain@cea.fr

<sup>b</sup> e-mail: christophe.baudet@hmg.inpg.fr

of unique wavevector  $\mathbf{k}$  (spatial band-pass filtering) without any resort to the Taylor hypothesis.

## 2 Acoustic scattering measurements

### 2.1 Acoustic scattering amplitude

It is now well established on both theoretical [3,13] and experimental grounds [4,14–18], that acoustic waves propagating in a turbulent medium can be scattered by vorticity fluctuations. As in any scattering experiments, it may be shown [13] that, due to the coherent average of the waves scattered by the vorticity distribution, the overall scattered amplitude  $p_{scatt}(t)$  is linearly related to the spatial Fourier transform of the vorticity field according to:

$$p_{scatt}(t) \propto \tilde{\omega}_{\perp}(\mathbf{k}, t) \cdot p_0(t) \quad (1)$$

where:

$$\tilde{\omega}_{\perp}(\mathbf{k}, t) = \iiint_{V_{scatt}} \omega_{\perp}(\mathbf{x}, t) e^{-i\mathbf{k}\cdot\mathbf{x}} d^3x \quad (2)$$

the scattering wavevector  $\mathbf{k}$  (momentum transfer) being a function of both the incoming sound frequency  $\nu_0$  and the scattering angle  $\theta$ :

$$\mathbf{k} = 4\pi\nu_0 \sin(\theta/2) / c \mathbf{x} \quad (3)$$

with  $c$  the sound speed. Equation (1) is derived from a Born approximation [18,19]. Note that only the component of the vorticity vector field, normal to the scattering plane, is involved in the scattered amplitude (index  $\perp$ ).

### 2.2 Acoustic scattering set-up

Experimentally, the scattering setup consists in a bistatic configuration (Fig. 2): a plane ultrasound wave  $p_0(t)$ , with frequency  $\nu_0$ , continuously insonifies the turbulent flow and the acoustic amplitude  $p_{scatt}(t)$ , scattered in the direction  $\theta$ , is recorded by a receiver over several integral time scales. Both acoustic transmitter and receiver work in a linear regime (they are phase sensitive). According to equation (1), a direct image of the spatial Fourier mode of the vorticity at wavevector  $\mathbf{k}$ , is obtained by a simple heterodyne demodulation providing a complex signal (phase and amplitude). We will now focus on the time behavior of the Fourier modes of vorticity  $\tilde{\omega}(\mathbf{k}, t)$ , as a function of the length scale parameter  $k$ . Although a Fourier mode is a complex quantity (as is the demodulated scattered signal), we will restrict ourselves to the amplitude of the signal:  $|\tilde{\omega}_{\perp}(\mathbf{k}, t)|$  hereafter noted  $\omega(k, t)$  for sake of simplicity.

### 2.3 Turbulent jet flow facility

We have investigated the statistical properties of a turbulent round air jet at room temperature, emerging

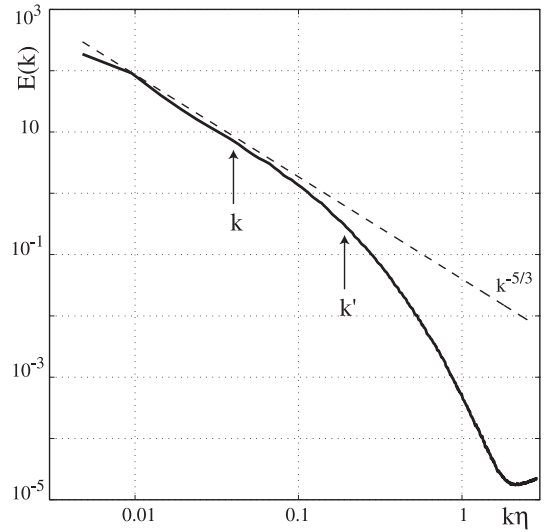


**Fig. 1.** Log-Log plot of the spatial kinetic energy spectrum  $E(k)$  in the turbulent round jet at  $R_{\lambda} \simeq 600$ . For the velocity signals obtained by hot-wire anemometry, the usual Taylor hypothesis has been used, to convert frequencies into wave-numbers  $k$ . Arrows point to the spatial wavenumbers  $k$  and  $k'$ , for which the instantaneous enstrophy and modal cross-correlation are displayed in Figures 3 and 7.

from a nozzle of diameter  $D = 0.12$  m. As sketched in Figure 2, the direction of the scattering wavevector  $\mathbf{k}$  is aligned with the mean flow velocity and the direction of the probed vorticity component is perpendicular to the jet axis. Throughout the experiment, the scattering angle is kept at a constant value and different wavevectors are analysed by varying the incoming sound frequency  $\nu_0$ , according to equation (3). As the scattering angle  $\theta$  is constant, one can show that, in our bistatic configuration, the spectral resolution is given by  $\delta k \sim V_{scatt}^{-1/3}$ , independent of the analysed wavenumber  $k$  [18]. The measurement volume  $V_{scatt}$  is defined by the intersection of the incident and detected acoustic beams and mainly depends on  $\theta$  and on the size of both acoustic transducers. In this study, the centre of the measurement volume is located 40 nozzle diameters downstream, in a region where turbulence is reasonably expected to reach a self-similar regime. With  $\theta = 40^\circ$  and a diameter of the circular transducers of 0.14 m, the linear extension of  $V_{scatt}$  is of the order of the integral length scale of the jet flow, estimated to  $L = 0.36$  m. The rms of the longitudinal velocity is  $u' = 1.2$  m/s, giving an integral time scale  $T_{int} = L/u' \simeq 0.3$  s. Additional flow parameters have been estimated, using conventional hot-wire anemometry [18]: the Taylor micro-scale is  $\lambda_T = 7.6 \times 10^{-3}$  m (Taylor-based Reynolds number  $R_{\lambda} \simeq 600$ ) and the Kolmogorov scale is  $\eta = 1.6 \times 10^{-4}$  m. Figure 1 displays a loglog representation of the spatial energy spectrum  $E(k)$ , versus the spatial wavenumber  $k$  (Taylor hypothesis), computed from longitudinal velocity measurements performed with a hot-wire located at the centre of the acoustic measurement zone.

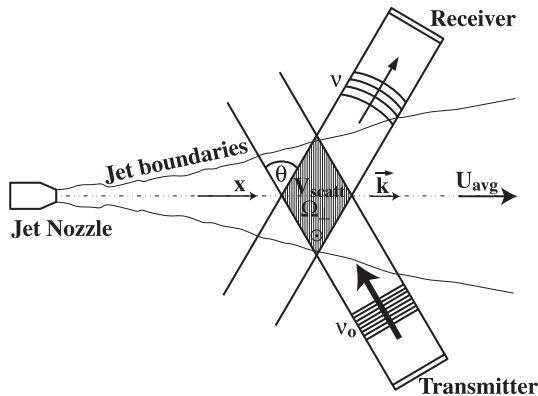


**Fig. 2.** Sketch of the experimental setup: turbulence is produced by a turbulent round jet at  $R_\lambda \simeq 600$ . The wavevector  $\mathbf{k}$  is parallel to the mean flow axis ( $x$ ) while the probed component of the vorticity vector field is perpendicular to the scattering plane.

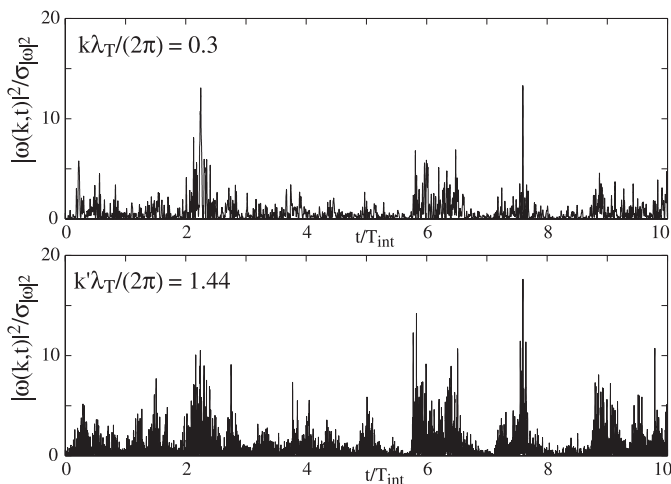


**Fig. 3.** Simultaneous recording, over ten integral time scales, of the temporal evolution of the instantaneous enstrophy  $|\omega(k,t)|^2$  at the two wavenumbers  $k\lambda_T/2\pi = 0.30$  (upper) and  $k'\lambda_T/2\pi = 1.44$  (lower).

**Table 1.** Jet flow characteristics.

$L_{int}$	$U_{avg}$	$u'_{rms}$	$R_\lambda$	$\lambda_{T_{ayl}}$	$\eta_{Kolm}$
0.36 m	6.3 m/s	1.2 m/s	600	$7.6 \times 10^{-3}$ m	$1.6 \times 10^{-4}$ m

### 3 Statistics of spatial Fourier modes

We have recorded, over long periods (typ.  $\geq 100T_{int}$ ), the evolution of the amplitude of the spatial Fourier modes  $\omega(k,t)$ , for several scattering wavevectors  $\mathbf{k}$  in the inertial range of the energy spectrum. Two samples, of the scattered acoustic intensities ( $\propto |\omega(k,t)|^2$ ) recorded simultaneously (see also below) for two spatial wavenumbers  $k\lambda_T/2\pi = 0.30$  and  $k'\lambda_T/2\pi = 1.44$ , at both ends of the investigated range of length scales, are displayed in Figure 3 (see Fig. 1 for their respective positions in the energy spectrum). The figure shows that both signals are organized in bursts of high enstrophy level, separated by

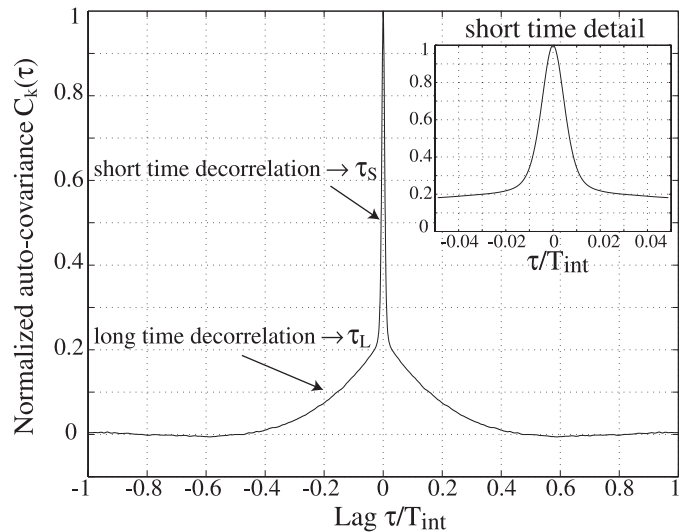


**Fig. 4.** Time auto-correlation function  $C_k(\tau)$  at wavenumber  $k\lambda_T/2\pi = 0.30$ . The global shape is similar for all analysed wavenumbers: a short-time decorrelation with characteristic time  $\tau_S$  (see insert for detail), followed by a much slower decrease, with characteristic time  $\tau_L$ . Here,  $\tau_S = 7.1$  ms and  $\tau_L = 45$  ms.

periods of lower activity. Note that on this simultaneous recordings, the bursts with a high enstrophy level appear at the same time for the two investigated wavenumbers. In addition to the aforementioned long time behaviour (the time interval between successive bursts is of the order of the integral time scale), the two signals also exhibit a spiky fine structure indicating a short time behaviour associated to the presence of finite duration events. Contrary to the long time behaviour, the short time dynamics seems to be scale dependent: the time duration is smaller for the larger wavenumber.

In order to investigate more quantitatively the temporal features of the signals, we have computed the time auto-correlation function of the time signals  $\omega(k,t)$ , collected at a fixed wavevector  $\mathbf{k}$ ,  $C_k(\tau) = \langle \omega(k,t)\omega(k,t-\tau) \rangle_t$  ( $\langle \cdot \rangle_t$  stands for the time average). A typical evolution of the normalized  $C_k(\tau)$  ( $C_k(0) = 1$ ), with respect to the time lag  $\tau$ , is sketched in Figure 4. Whatever the turbulent scale  $k$ , the same global shape is found, exhibiting two different and well separated characteristic times. For time lags close to zero, one observes a rapid decrease, with a more or less Gaussian shape. At larger time lags, a much slower decrease is visible, up to the integral time  $T_{int}$ , with a roughly exponential behavior.

Although such a Gaussian shape at short times has been predicted in some theoretical models [20, 21], the long time behaviour does not seem to have ever been reported. We quantitatively estimate the short time  $\tau_S$ , by measuring the half amplitude width ( $C_k(\tau_S) = 1/2$ ) in the small lags region (cf. Fig. 5). As usually done for the velocity auto-correlation, the characteristic time  $\tau_L$  of the long time behaviour is estimated by computing the area under the correlation, for time lags larger than  $\tau_S$  (following an

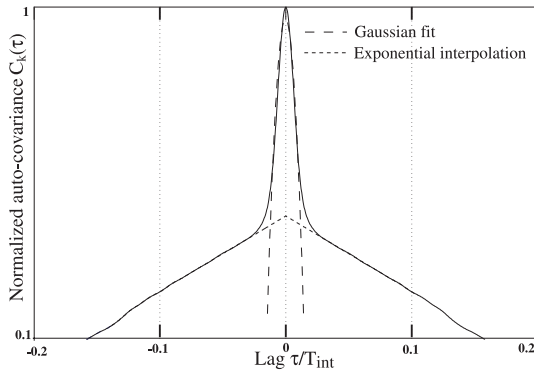


**Fig. 5.** Sketch of the Gaussian fit (long dashed line) and of the exponential extrapolation (short dashed line) towards the zero-lag used to compute the short time  $\tau_S$  and the long time  $\tau_L$  from modal auto-covariance estimates.

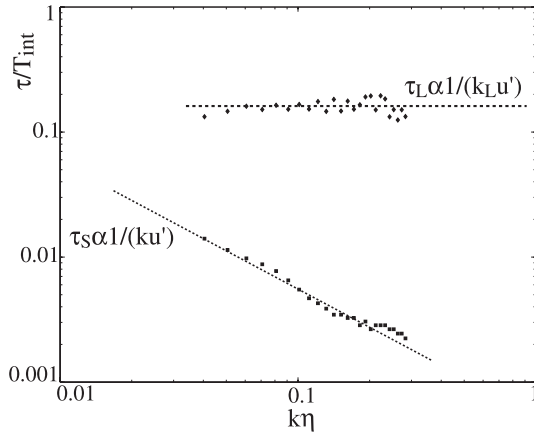


**Fig. 6.** Log-log plot of the evolution of the two characteristic time scales of Fourier modes in turbulence.

exponential extrapolation towards the zero-lag, to get rid of the short time scale contribution, see Fig. 5).

We now turn to the scaling of both characteristic times with the wavenumber  $k$ . By tuning the incoming sound frequency ( $15 \text{ kHz} \leq \nu_o \leq 170 \text{ kHz}$ ), we have successively probed a decade of wavenumbers  $k$ , spanning the inertial range of the turbulent flow down to the dissipative range ( $0.23 < k\lambda_T/2\pi < 2.6$ ). Figure 6 clearly reveals two different behaviours:  $\tau_S$  is scale dependent while  $\tau_L$  is not. Systematic studies, performed in various flow configurations (velocity  $u'$  and integral scale  $L$ ) gave us reliable results for both times.

### 3.1 Sweeping decorrelation

As for the short time  $\tau_S$ , it decreases with  $k$  following the power law  $\tau_S \propto (ku')^{-1}$ . In our experiments, the proportionality constant is about 1, and slightly decreases with the Reynolds number. Such a scaling law, involving the root mean square velocity (a large scale quantity), is usually ascribed to a sweeping effect associated with the random advection of the vorticity field by the large scale velocity fluctuations. According to the Kolmogorov phe-

nomenology (global scale invariance), one would expect a dynamic scaling of the modal correlation  $C_k(\tau)$  of the form  $\tau_{\text{eddy}}(k) \propto (ku(k))^{-1} \propto k^{-2/3}$ , where  $\tau_{\text{eddy}}(k)$  is the characteristic decay time of a turbulent eddy at scale  $k$  (eddy turn over time). Actually, the decay time must be compared to the sweeping time  $\tau_{\text{sweep}}(k) \propto (ku(L))^{-1}$  over which any spatial Fourier mode will be distorted by the random advection term entering the dynamical evolution of the vorticity field in the Fourier domain [12, 25]. For scales in the inertial range:  $\tau_{\text{sweep}}(k) \ll \tau_{\text{eddy}}(k)$ , hence the dynamical evolution of the spatial Fourier modes is dominated by the sweeping, in agreement with our experimental results. Note, however, that the Kolmogorov scaling  $\tau_{\text{eddy}}(k) \propto k^{-2/3}$  is recovered for the time-correlation of the modal amplitudes in the so-called *Shell Models* of turbulence, known to be free from sweeping effects [7].

### 3.2 Long-time memory and intermittency

Let us now turn to the large time  $\tau_L$ : as we have checked extensively (by varying acoustic as well as flow conditions separately)  $\tau_L$  is constant over the whole range of investigated scales:  $\tau_L \propto (k_L u')^{-1}$  (where  $k_L = 2\pi/L$  is the large scale wavenumber). As a whole, the coexistence of both the scale invariant long-time behaviour and the scale dependent short time one, implies that it is not possible to collapse all the correlation functions onto a single one. From a statistical viewpoint (dynamic multi-scaling [7]), this result evidences a breaking of self-similarity. We wish to stress the fact that this feature is a direct consequence of the existence of a scale invariant long-time behaviour. Indeed, it is independent of the short time scaling exponent, whether related to sweeping effects ( $\tau_S \propto k^{-1}$ ) or Kolmogorov decay time ( $\tau_S \propto k^{-2/3}$ ). It is worth mentioning, at this point, that we have also evidenced some influence of the spatial intermittency of turbulence in the Fourier domain [27]. Spatial intermittency is manifested by a significant dependence of the statistics of each spatial Fourier mode (probability density function of the amplitude) on the spatial extension  $V_{\text{scatt}}^{-1/3}$  of the experimental setup with respect to the integral length scale  $L$  of the turbulent flow.

## 4 Non-local interactions

The scattering technique allows simultaneous recordings of two distinct spatial Fourier modes  $k$  and  $k'$ . By computing the time cross-correlation function between two distinct modes, we investigate the dynamics of more or less non-local (in the Fourier domain) interactions between spatial Fourier modes. Since local interactions have been analysed in a previous experiment [17], we focus here on non-local interactions (finite spectral gap  $k - k'$ ). Provided the spectral gap  $k - k'$  is large enough, such measurements can be performed by driving a single transmitter with the sum of two sine waves with the appropriate frequencies  $\nu_o$

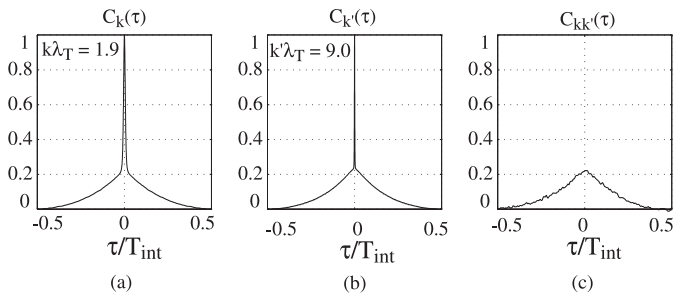


**Fig. 7.** plots of time correlation functions: (a) auto-correlation  $C_k(\tau)$  for  $k\eta = 0.04$  (as in Fig. 4); (b) auto-correlation  $C_{k'}(\tau)$  for  $k'\eta = 0.19$ ; (c) cross-correlation  $C_{kk'}(\tau)$  between the two foregoing Fourier modes.

and  $\nu'_o$  (Eq. (3)). The scattered pressure signals, around each incoming frequency, can be easily separated by means of two simple band-pass filtering operations. To avoid spurious interference effects, the same investigation could also be performed by using a second pair of transducers defining a second independent scattering channel as in [17]. However, the single pair configuration presents the advantages of a better wavevectors alignment as well as the best possible measurement volumes matching. Actually, we have carefully checked that both setups give the same results.

From two *synchronous* time series (at  $k$  and  $k'$ ), with a well controlled spectral gap  $k - k'$ , we have computed the cross-correlation function  $C_{k,k'}(\tau) = \langle \omega(k, t) \omega(k', t - \tau) \rangle_t$ . A typical example of this cross-correlation is displayed in Figure 7c. We have also represented in Figure 7a (resp b), the auto-correlation function of the two spatial Fourier modes with wavenumbers  $k$  (resp.  $k'$ ). As an illustration of the scale independence of the long time  $\tau_L$ , Figure 7a (resp b) shows the identity of the long time part of the correlation (even superposable). The cross-correlation displayed in Figure 7c, is also identical to both auto-correlations, as regards the long time part. The only difference lies in the absence of the rapid decay at small time (previously ascribed to sweeping effects). Note that we have shown in a previous study [17] that significant cross-correlation levels are recovered, even at small time lags, for small enough spectral gaps (typ. for  $k - k' = O(2\pi/L_{int})$ ). The significant cross-correlation level (about 20%) between two spatial Fourier modes  $k$  and  $k'$ , irrespective of the spectral gap  $k - k'$ , implies a strong statistical dependence between scales, corresponding to non-local interactions. A similar result has been recently reported, in a direct numerical simulation (DNS) of the so called turbulent Taylor-Green vortex flow, with comparable Reynolds numbers ( $R_\lambda \simeq 800$ ) [26]. Actually, in their DNS investigation, these authors focused on statistics of the average energy transfer rate  $T_2(k, k')$  between Fourier modes in wavenumber shells  $k$  and  $k'$ . Whatever the scale  $k$ , they observe that it predominantly exchanges energy with modes  $k'$  lying in a band of constant width  $k_o$  around  $k$ . They conclude that, as *the integral length scale  $k_o^{-1}$  is remembered even deep inside the constant flux inertial range, the energy transfer processes are not*

*self-similar*. In some way, our experimental results, well agree with the results of the DNS, albeit in the time domain: the temporal fluctuations of the large scales affect the time dynamic of all scales in the inertial range according to some kind of memory effect. Moreover, as far as this long time driving process is concerned, the significant cross-correlation level suggests that all scales are *instantaneously* driven by the same large-scale process.

## 5 Conclusions

To summarize, acoustic scattering allows the direct spectral probing, continuously in time, of spatial Fourier modes of one component of the vorticity vector field. Thanks to a good spectral resolution, the proper selection of a well defined wavevector  $\mathbf{k}$  of the turbulent flow results in an unambiguous separation of the spatial and time features of the turbulent vorticity dynamic. As a first result, the short time scaling of the modal correlation is consistent with sweeping effects. This short time scaling, involving the fluctuating velocity, can be understood as the consequence of the differential advection between different parts of spatially extended vorticity structures (coherent structure). This differential advection, resulting in strong deformations of the coherent structure (bending and strain), is expected to be responsible for significant redistribution of the enstrophy amplitude over neighbouring spatial wavevectors. Actually, this process, involving large scale velocity gradients, is very similar and reminiscent of the turbulent dispersion of a passive scalar. Second, a long-time correlation, over time lags up to the integral time scale, indicates a significant statistical dependency between scales. In recent numerical investigations [6], relying on Direct Numerical Simulations of modulated turbulence, A.K. Kuczaj and co-workers have clearly demonstrated that large scale modulations of the energy injection rate can significantly affect the time evolution of both large and small scale quantities (eg. total energy and Taylor Reynolds number). Accordingly, the persistent long time behaviour of the amplitudes of Fourier modes (whatever the wave vector), reported here, could possibly be the signature of some kind of memory of the temporal fluctuations of the rate of energy injection at large scale. Our results, suggest that the turbulent Fourier modes are driven by two distinct processes, a rapid one which is local in  $k$ -space and a much slower one, involving non-local interactions. As far as coherent structures are concerned, it has been reported in various turbulent flow situations (jet, closed flow between rotating disks) that coherent vorticity structures exhibit a filamentary shape with a sharp space localization (implying some kind of delocalization in the Fourier domain), with axial dimensions of order the integral scale and life time of order the integral time scale. Thus, such spatio-temporal features of the coherent structures, observed in both experiments and numerical simulations, could account for the complex behaviour of the modal auto and cross correlations. We propose to interpret the lack of self-similarity of the modal time correlations as the signature of some kind of temporal

intermittency (in addition to the usual small scale spatial intermittency [27]). Note that, as we have observed similar statistical behaviours at smaller Reynolds numbers (in a grid turbulence at  $Re_\lambda \simeq 100$ ), as well as at much higher Reynolds numbers (up to  $Re_\lambda \simeq 6000$ , in a cryogenic Helium jet facility at CERN [28]), we believe that they could correspond to generic features of turbulence.

This work is fully supported by the French Ministère de la Recherche and Université Joseph Fourier (PPF plateforme expérimentale de spectroscopie acoustique multi-échelles). We thank Jean-Paul Barbier-Neyret and Joseph Virone for their valuable technical help.

## References

1. U. Frisch, *Turbulence, The Legacy of A.N. Kolmogorov* (Cambridge University Press, Cambridge, 1995)
2. A.N. Kolmogorov, Dokl. Akad. Nauk. SSSR **30**, 299 (1941), reprinted in Proc. R. Soc. Lond. A **434**, 9 (1991)
3. R.H. Kraichnan, J. Acoust. Soc. Am. **25**, 1096 (1953)
4. C. Baudet, S. Ciliberto, J.F. Pinton, Phys. Rev. Lett. **67**, 193 (1991)
5. A.N. Kolmogorov, J. Fluid Mech. **13**, 82 (1962)
6. A.K. Kuczaj, B.J. Geurts, D. Lohse, Europhys. Lett. **73**, 851 (2006)
7. S. Dhar, A. Sain, R. Pandit, Phys. Rev. Lett. **78**, (1997) 2964; D. Mitra, R. Pandit, Physica A: Statistical Mechanics and its Applications **318**, Issues 1-2 (2003) 179; D. Mitra, R. Pandit, Phys. Rev. Lett. **93**, 024501 (2004)
8. S. Chen, R.H. Kraichnan, Phys. Fluids A **1**, 2019 (1989)
9. Y. Kaneda, T. Ishihara, K. Gotoh, Phys. Fluids **11**, 2154 (1999)
10. M. Nelkin, M. Tabor, Phys. Fluids A, **2**, 81 (1990)
11. B. Castaing, Eur. Phys. J. B **29**, 357 (2002)
12. R.H. Kraichnan, J. Fluid Mech. **83**, 349 (1977)
13. F. Lund, C. Rojas, Physica D **37**, 508 (1989)
14. M.A. Kallistratova, Dokl. Akad. Nauk. SSSR **125**, 69 (1959)
15. C.M. Ho, L.S.G. Kovàsznay, J. Acoust. Soc. Am. **60**, 40 (1976)
16. B. Deroncourt, J.-F. Pinton, S. Fauve, Physica D **117**, 181 (1998)
17. C. Baudet, O. Michel, W.J. Williams, Physica D **128**, 1 (1999)
18. C. Poulain, N. Mazellier, P. Gervais, Y. Gagne, C. Baudet, Flow, Turb. Comb. **72**, 245 (2004)
19. As a consequence of the Born approximation, equation (1) is valid in the far field limit, at low Mach numbers  $u/c$  and low acoustic intensity such that  $v \ll u \ll c$ , where  $v$  is the typical amplitude of the acoustic velocity fluctuations
20. W. Heisenberg, Z. Phys. **124**, 628 (1948)
21. R.H. Kraichnan, J. Fluid Mech. **5**, 497 (1959)
22. A.A. Praskovsky et al., J. Fluid Mech. **248**, 493 (1993)
23. H. Tennekes J. Fluid Mech. **67**, 561 (1975)
24. V. Yakhot et al., Phys. Fluids A **1**, **2**, 184 (1989)
25. P.A. O’Gorman, D.I. Pullin, J. of Turb. **5**, 035 (2004)
26. A. Alexakis, P.D. Mininni, A. Pouquet, Phys. Rev. Lett. **95**, 264503 (2005)
27. L. Chevillard, N. Mazellier, C. Poulain, Y. Gagne, C. Baudet, Phys. Rev. Lett. **95–20**, 200203 (2005)
28. S. Piétropinto, C. Poulain, C. Baudet, B. Castaing, B. Chabaud, Y. Gagne, P. Gervais, B. Hébral, Y. Ladam, P. Lebrun, O. Pirotte, *Very high Reynolds turbulence with low-temperature gaseous helium*, Proceedings of the 9th European Turbulence Conference, Southampton UK 279 (2002)